Psychological Review
2010, Vol. 117, No. 4, 1267–1274

0033-295X/10/$12.00 DOI: 10.1037/a0020793

Gradual Growth Versus Shape Invariance in Perceptual Decision Making

Jeffrey N. Rouder
University of Missouri

Yu Yue
City University of New York, Baruch College

Paul L. Speckman, Michael S. Pratte, and Jordan M. Province
University of Missouri

A dominant theme in modeling human perceptual judgments is that sensory neural activity is summed or integrated until a critical bound is reached. Such models predict that, in general, the shape of response time distributions change across conditions, although in practice, this shape change may be subtle. An alternative view is that response time distributions are shape invariant across conditions or groups. Shape invariance is predicted by some race models in which the first of several parallel fibers to communicate the signal determines the response. We competitively assess a specific gradual growth model, the one-bound diffusion model, against a natural shape-invariant competitor: shape invariance in an inverse Gaussian distribution. Assessment of subtle shape change versus shape invariance of response time distributions is aided by a Bayesian approach that allows the pooling of information across multiple participants. We find, conditional on reasonable distributional assumptions, subtle shape changes in response time that are highly concordant with a simple diffusion gradual growth model and discordant with shape invariance.

Keywords: information accumulation, perception, Bayesian models

This theoretical note concerns how people and animals make quick perceptual judgments. The dynamics of these judgments are typically modeled as a process of gradual growth. Activation, be it latent or neural, grows gradually until some criterial value is reached, and then a response is produced. This theme of gradual growth is fundamental in many behavioral and neurological accounts of perceptual decision making. Selected examples include the models developed in Brown and Heathcote (2005), Hanes and Shall (1996), Huk and Shadlen (2005), Morton (1969), Ratcliff (1978), Reddi and Carpenter (2003), and Usher & McClelland (2001). Perhaps the most popular gradual growth model is Ratcliff's (1978) diffusion model. A simple version of the model is shown in Figure 1.[1] A sample path of activation is shown as the jagged gray line. A response is produced when the path is absorbed at the *bound* (denoted with a thick horizontal line). The parameters of the model are the *drift rate*, or average rate of activation gain per unit time (shown as an arrow), and the criterial bound. The drift rate corresponds to the strength of the stimulus, with stronger stimulation driving quicker growth (e.g., Ratcliff & Rouder, 1998). Typically, a shift or offset is added to the absorption time to model the effects of *nondecision processes*, such as encoding the stimulus or executing the response (Laming, 1968).

Although gradual growth models are popular and appealing, there are alternatives without recourse to growth. The one we explore is *shape invariance*. Figure 2 depicts properties of shift, scale, and shape in distributions. Shape refers to properties of distributions that are indexed by moments higher than variance: for example, skew and kurtosis. Many candidate response time (RT) distributions may be parameterized with explicit shift, scale, and shape parameters; examples include the lognormal, gamma, and Weibull families. The principle of shape invariance is that although shift and scale may vary across people, tasks, or conditions, shape may not.

The power of shape invariance is seen by consideration of a formal definition. Let $T_1, T_2, \ldots, T_N$ be a set of theoretical RT distributions. This set could be over conditions, people, or even condition-by-person combinations. Shape invariance implies that $T_i = \psi_i + \theta_i Z$, where Z is a canonical distribution that does not change across the set and ψ_i and θ_i are parameters that denote shift and scale, respectively, for the ith distribution. The key constraint is that all RT distributions in the set are shifted and scaled versions of the same canonical form. Shape invariance, should it hold, is a striking regularity in data and an appropriate target for theoretical explanation.

Jeffrey N. Rouder, Michael S. Pratte, and Jordan M. Province, Department of Psychological Sciences, University of Missouri; Yu Yue, Zicklin School of Business, City University of New York, Baruch College; Paul L. Speckman, Department of Statistics, University of Missouri.

This research is supported by Grant SES-0095919 from the National Science Foundation. We thank Robert Paterson, Lindsey Peeples, Michael Cusumano, and Elliott Cade for help in running the reported experiment. We are grateful for helpful comments from Scott Brown, E.-J. Wagenmakers, and Marius Usher.

Correspondence concerning this article should be addressed to Jeffrey N. Rouder, Department of Psychological Sciences, 210 McAlester Hall, University of Missouri, Columbia, MO 65211. E-mail: rouderj@missouri.edu

[1] Activation x at time t is modeled as a Wiener diffusion process. The partial differential equation describing the density of activation, f, is $\frac{\partial f(x,t)}{\partial t} = -\nu \frac{\partial f(x,t)}{\partial t} + \sigma^2 \frac{\partial^2 f(x,t)}{\partial x^2}$, where ν and σ are called the *drift rate* and the *coefficient of drift*, respectively. For modeling perceptual judgments, the activation x is assumed to be latent. Consequently, σ serves as the scale of activation and is set to 1.0 without any loss of generality.

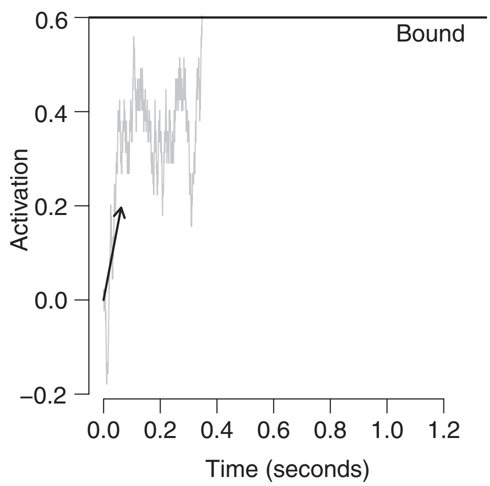

Figure 1. A one-bound diffusion process. The light gray jagged line shows a sample activation path; the arrow denotes the drift rate.

Shape invariance, although not identified as such, has been integral to a number of perspectives. From a processing perspective, Logan (1992) and Ulrich and Miller (1993) noted that shape invariance holds across some parallel-processing models. Logan (1992), for example, posited that RT reflects the first time when one of many competing parallel processes finishes. Responses are speeded when there are more competing processes. According to these models, the effect is in scale, such as in the middle panel of Figure 2, rather than in shift or shape. An alternative account of shape invariance is provided by Myerson and colleagues (Myerson, Hale, Wagstaff, Poon, & Smith, 1990; Myerson, Hale, Zheng, Jenkins, & Widaman, 2003), who advocate a generalized slowing view of the effects of cognitive aging. According to Myerson and colleagues, RT is the sum of several latent components. Aging proportionately lengthens each of these components, and this proportionality results in shape invariance. From a statistical and psychometric perspective, shape invariance is useful for measuring various aspects of performance (Rouder, Lu, Speckman, Sun, & Jiang, 2005; Van Breukelen, 2005). It serves as a more realistic assumption than the variance homogeneity implicit in conventional analysis of variance (ANOVA) and regression models.

Evidence for Gradual Growth and Shape Invariance

A number of behavioral lines of evidence support gradual growth models. Several studies have shown that specific gradual growth models, such as Ratcliff's diffusion model or Brown and Heathcote's linear ballistic accumulator, can account for RT and accuracy data across a number of tasks, age groups, and conditions (e.g., Brown & Heathcote, 2005; Gomez, Ratcliff, & Perea, 2007; Ratcliff, Gomez, & McKoon, 2004; Ratcliff & Rouder, 2000; Spaniol, Voss, & Grady, 2008; Thapar, Ratcliff, & McKoon, 2003). Moreover, researchers have demonstrated selective influence in which manipulations hypothesized to affect only prespecified parameters indeed do so (e.g., Voss, Rothermund, & Voss, 2004). In sum, the evidence for various gradual growth models in the literature is plentiful and varied.

Although shape invariance has not received the considerable attention that gradual growth has, it too seems plausible. It has long been noted that histograms of RT distributions seemingly have a canonical shape characterized by unimodality and a long right tail (Luce, 1986). On a more formal level, two natural consequences of shape invariance tend to hold in the empirical distributions. One consequence is that the standard deviation of RT tends to increase linearly with the mean, and this property tends to hold fairly robustly in data (Luce, 1986; Wagenmakers & Brown, 2007). The second natural consequence of shape invariance is that quantile–quantile (QQ) plots of RT distributions are straight lines with no curvature. Figure 3 shows empirical QQ plots from four studies in which stimulus strength was manipulated. The lines, which describe the points to high precision, are best-fitting linear regression lines.

How can the evidence for gradual growth models and for shape invariance be reconciled? Extant gradual growth models predict shape changes in RT distributions across strength manipulations. The shape changes implied by these models, however, are often quite small and fairly subtle. For example, Ratcliff, Spieler, and McKoon (2000) showed that the diffusion model can mimic the linear QQ plots provided in Smith and Brewer (1995). One reason the diffusion model mimics shape invariance is the use of *across-trial variability* in addition to *within-trial variability*. The trajec-

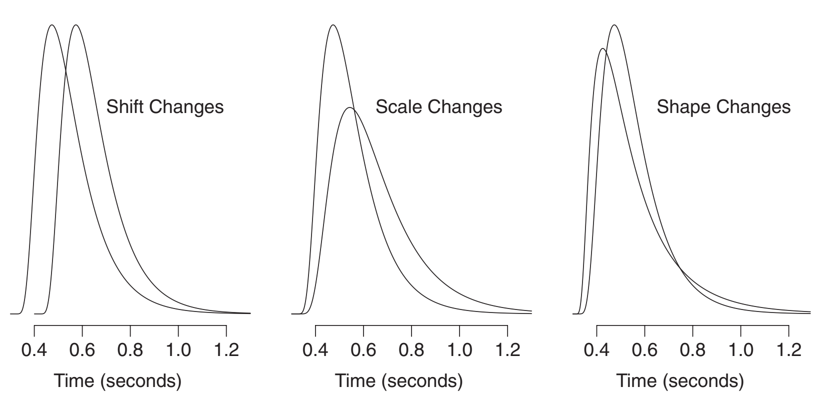

Figure 2. Effects of varying shift, scale, and shape parameters in a shift–scale–shape distribution family.

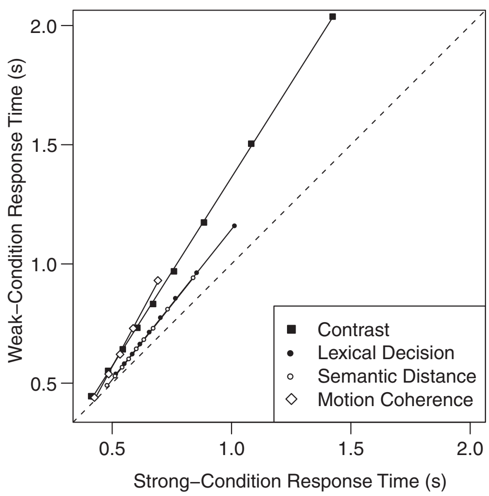

Figure 3. Quantile–quantile plots from four experiments are straight lines, consistent with shape invariance. The sequence labeled *Contrast* is from Ratcliff and Rouder's (1998) Experiment 1, in which participants judged whether a light or a dark square differed in brightness from a gray background. In the strong and weak conditions, squares differed markedly or subtly from the background, respectively. The sequence labeled *Lexical Decision* is from Gomez, Ratcliff, and Perea (2007), in which participants performed a lexical decision task. Words with Kuœra–Francis frequencies between 1 and 6 and between 7 and 20 made up the weak and strong conditions, respectively. The sequence labeled *Semantic Distance* is from Rouder, Lu, Speckman, Sun, and Jiang (2005), in which participants judged whether digits were less than or greater than 5. The digits *2* and *8* make up the strong condition; digits *4* and *6* make up the weak one. The sequence labeled *Motion Coherence* is from Ratcliff and McKoon (2008, Figure 8) in which participants identified the direction of coherent motion. High-coherent motion and low-coherent motion (Conditions 6 and 1, respectively, in that article) made up the strong and weak conditions, respectively. All points are averaged quantiles (Jiang, Rouder, & Speckman, 2004) or Vincentiles (Ratcliff, 1979). The lines are best-fitting linear regression lines.

tory of Figure 1 shows within-trial variability. Across-trial variability refers to variations in parameters (drift rate, bound, and shift) across trials. The addition of across-trial variation has proved necessary to account for fine details of the joint distributions of RT and accuracy (Ratcliff & Rouder, 1998; Ratcliff, Van Zandt, & McKoon, 1999). These additional across-trial variabilities in primary parameters tend to attenuate predicted shape differences across conditions.

We find the gradual growth account of approximate shape invariance to be unsatisfying. Shape invariance in distribution is a simple principle that may be accounted for with two free parameters: shift and scale. The gradual growth account is far more complex. First, it predicts only approximate rather than actual shape invariance. Second, it does so with recourse to three primary parameters (bound, rate of growth, shift) in conjunction with across-trial variabilities in these parameters. In sum, although gradual growth models may mimic shape invariance, they do so through increased flexibility rather than through parsimony. In our view, shape invariance, should it hold, serves as a foundational empirical phenomenon suitable for direct and parsimonious explanation.

Competitively Testing Gradual Growth Versus Shape Invariance

Assessing shape invariance is difficult. For example, it is not obvious how to statistically test the linearity of averaged quantiles in the QQ plots of Figure 3. Rouder, Speckman, Steinley, Pratte, and Morey (2010) provided a nonparametric bootstrap test of shape invariance, but it is of low power and cannot differentiate shape invariance from the subtle changes in shape implied by most gradual growth models. The approach we take here is to construct a parametric test between two alternative hypotheses: (a) Shape is invariant across a strength manipulation versus (b) shape changes with strength as predicted by the one-bound gradual growth model of Figure 1. Both of these hypotheses are implemented in a common statistical distributional family, the *inverse Gaussian,* which is discussed subsequently.

The test is based on manipulating stimulus strength across conditions. Participants were presented with Gabor patches with orientation tilted from vertical (see Figure 4), and they judged whether the tilt was leftward or rightward. Although rightward tilts are not shown in Figure 4, they occurred with equal frequency in the reported experiment. The magnitude of tilt, whether leftward or rightward, was varied, with some patches having an obvious tilt (e.g., Patch I in Figure 4) and other having a more subtle one (e.g., Patch II in Figure 4). The tilt-angle magnitude served as a strength variable. In the reported experiments, tilt angle was randomly varied across trials; hence, participants had no advanced knowledge of the stimulus and could not vary their criterial settings with stimulus strength. Therefore, in the gradual growth account, stimulus strength affects drift rate but not bound. We term this property *bound invariance*.

Bound invariance places constraints on RT distributions. As the drift rate decreases, distributions not only increase in scale but become more skewed. Figure 4 provides an example. Patch I is more extreme in tilt and corresponds to a drift rate that is higher than that for Patch II. The corresponding RT distributions are shown in the right panel as Curves i and ii. Hence, Distributions i and ii are bound invariant. They are not, however, shape invariant. Distribution iii is shape invariant with Distribution i but not with Distribution ii. The difference between Distributions ii and iii shows the correlates of bound invariance and shape invariance, respectively. This difference, although subtle, is discernible in the experiment we report.

The key question is whether the data are better described as bound invariant or, alternatively, shape invariant. The three-parameter inverse Gaussian distribution is ideal for answering this question. On the one hand, the inverse Gaussian distribution describes RT distributions from a one-bound diffusion process (Chhikara & Folks, 1989). The probability density function of the inverse Gaussian distribution is

$$f(t;\psi,\nu,\lambda)=\frac{\lambda}{\sqrt{2\pi}}(t-\psi)^{-3/2}\exp\left(-\frac{[\lambda-\nu(t-\psi)]^2}{2(t-\psi)}\right),\quad t>\psi;\ \nu,\lambda>0. \qquad (1)$$

Parameters ψ, ν, and λ denote the shift, drift rate, and bound, respectively. On the other hand, the inverse Gaussian distribution may be reparameterized in a shift–scale–shape form. Let ν_i and λ_i denote the drift rate and bound of the inverse Gaussian distribu-

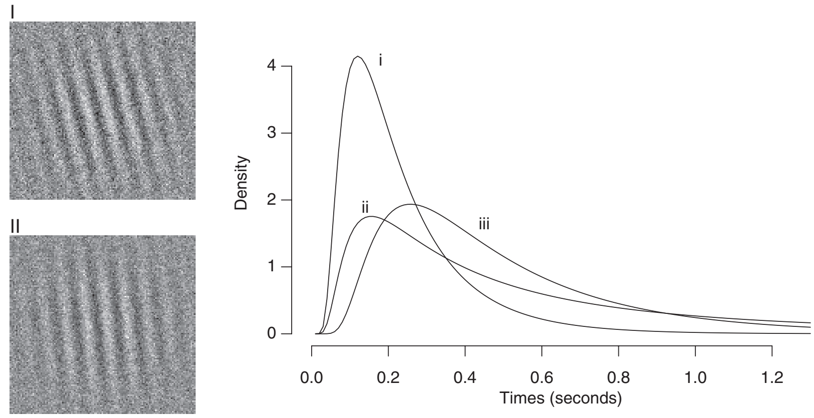

Figure 4. Stimuli and distributional predictions. Left: Patch I and Patch II have an obvious and a subtle leftward tilt, respectively. Right: Distributional correlates of shape and bound invariance. Distributions i and ii are the correlates of bound invariance; Distributions i and iii display shape invariance.

tion, respectively, for the *i*th tilt-angle condition. It is straightforward to show that the quantities

$$\theta_i = \lambda_i/\nu_i, \tag{2}$$

$$\beta_i = \lambda_i\nu_i, \tag{3}$$

are the scale and shape of the distribution, respectively.[2] This reparameterization provides the key to testing bound and shape invariance. Bound invariance implies that λ_i, the bound, is constant across changes in tilt angle; that is, $\lambda_i = \lambda$. Shape invariance, in contrast, implies that β_i, the shape parameter, is constant across changes in tilt angle; that is, $\beta_i = \beta$. Assessment of these invariances is aided by noting that Equations 2 and 3 imply

$$\log\theta_i = \log\lambda_i - \log\nu_i, \tag{4}$$

$$\log\beta_i = \log\lambda_i + \log\nu_i. \tag{5}$$

Bound invariance occurs if $\log\beta_i = -\log\theta_i + c_0$, where $c_0 = 2\log\lambda$ is a constant across conditions.[3] Hence, bound invariance predicts that the relationship between log shape and log scale follows a straight line with slope -1.0. Shape invariance, in contrast, implies that $\log\beta_i$ does not vary with $\log\theta_i$. Clearly, both relationships cannot hold simultaneously.

The fact that both shape invariance and bound invariance can be expressed as reparameterizations of the inverse Gaussian distribution greatly facilitates the comparison of the two. In analysis, we let shape and scale be free parameters that may take on any values. We simply assess whether the relationship between $\log\beta$ and $\log\theta$ has a slope closer to -1 or 0. Had there been no common distribution for bound and shape invariance, the comparison would have been more difficult.

There are two significant limitations to this approach. The first is the assumption that RT follows an inverse Gaussian distribution: If the data deviate grossly from the inverse Gaussian distribution, then the test is inappropriate. Hence, we assess how well the inverse Gaussian distribution describes the data. The second limitation of the current approach is that although the task is a two-choice task, the model assumes only correct responses are possible. Ordinarily, two-choice tasks are modeled with two-bound diffusion processes (e.g., Ratcliff & Rouder, 1998). The two-bound diffusion model, however, cannot be reparameterized conveniently with scale and shape parameters and is, consequently, not suitable for assessing shape invariance. Fortunately, the two-bound diffusion model may be closely approximated by the one-bound diffusion model in Figure 1 when task accuracy is high, but not necessarily otherwise (Matzke & Wagenmakers, 2009). Hence, the usefulness of the inverse Gaussian model is conditional on highly accurate performance. The following experiment provides for large RT effects with high levels of accuracy.

Method

Participants

Fifty-eight students in an introductory psychology course at the University of Missouri served as participants in exchange for course credit.

Stimuli

Stimuli were the supposition of Gabor patches and pixelated noise (see Figure 4). The Gabor patches were composed of 2-D sinusoidal gratings with different tilt angles corresponding to different *y*-axis frequencies of $\pm 0.4°$, $\pm 0.2°$, and $\pm 0.15°$ per pixel. The *x*-axis frequency was fixed at 5.7° per pixel. The resulting six tilt angles were $\pm 4°$, $\pm 2°$, and $\pm 1.5°$. These gratings were mod-

[2] The density for a shift–scale–shape family may be expressed as $f(t; \psi, \theta, \beta) = \frac{1}{\theta} g(z; \beta)$, where $z = (t - \psi)/\theta$ is a standardized score; g is a density function; and ψ, θ, and β are shift, scale, and shape parameters, respectively. To see that the inverse Gaussian distribution follows a shift–scale–shape parameterization, substitute Equations 2 and 3 into Equation 1. The result is $f(t; \psi, \theta, \beta) = \frac{1}{\theta} g(z; \beta)$, where $g(z; \beta) = \sqrt{\frac{\beta}{2\pi}} z^{-3/2} \exp\left(-\frac{\beta(z-1)^2}{2z}\right)$. Hence, ψ, θ, and β serve as shift, scale, and shape parameters, respectively.

[3] Equations 4 and 5 show that the two parameterizations are 45° rotations of each other.

ulated by a two-dimensional Gaussian filter that had a full width at half maximum dispersion of 83 pixels in each direction. These gratings were of high contrast with peak-to-peak amplitudes corresponding to approximately three quarters of the luminance range of the CRT displays. The pixelated noise was of low power (approximately one tenth that of the gratings) and was added to avoid any aliasing of line segments. Consequently, the gratings were clearly visible; the tilt angle, however, was subtle (especially for the $\pm 1.5°$ tilts).

Design

The experiment was a 2×3 within-subject balanced factorial design with tilt direction and tilt magnitudes serving as factors. All combinations of factors occurred equally often across the experiment for each participant.

Procedure

Each trial began with the presentation of noise. After a 1-s foreperiod, the Gabor patch was superimposed on the noise. The patch and noise were displayed until response. Participants judged the orientation of the patch by depressing the *z* and / keys to indicate left and right orientations, respectively. Auditory feedback about the correctness of each judgment was provided by either a high-pitched or a low-pitched tone for correct and error responses, respectively. To elicit high accuracy, we made sure error responses were followed by a 2-s delay in which the participants were reminded to be accurate. Participants observed 9 blocks of 80 trials each and took short breaks between blocks. The entire session lasted about 45 min.

Results

Figure 5A shows the resulting RTs for correct responses as a function of tilt angle and amount of practice. As can be seen, participants improved in speed over the first third of the experiment and were relatively stable thereafter. Hence, only data from the later two thirds were retained for analysis. Additional trials discarded include all errors (3%), all responses with RT longer than 5 s (1%), trials following errors (3%; see Rabbit, 1966, for a justification), and trials following breaks (1%). Resulting mean RT as a function of condition is shown in Figure 5B. The magnitude of tilt angle had a large 150-ms effect, $F(2, 114) = 319.4$, $p < .05$. Leftward tilts were responded to more quickly than rightward tilts, $F(1, 57) = 26.4$, $p < .05$, and the interaction between direction and magnitude was significant, $F(2, 114) = 8.9$, $p < .05$. We interpret these effects subsequently within the context of the models. Accuracies were quite high, averaging .94, .97, and .99 for the 1.5°, 2°, and 4° tilts, respectively. Leftward tilts were responded to slightly more accurately than were rightward tilts (.97 vs. .96, respectively), indicating that quicker responses to leftward tilts were not the result of a speed–accuracy trade-off.

The critical questions are about bound and shape invariance. Our approach is to fit a general inverse Gaussian model in which shape and scale are free to vary across participants and strength levels. This approach is equivalent to allowing drift rate and bound to vary across participants and strength levels. Consequently and importantly, neither shape invariance nor bound invariance is assumed.

The Appendix describes the details of the statistical model. As mentioned previously, the analysis is conditional on the good fit of the inverse Gaussian distribution. Figure 6A shows the adequacy of the inverse Gaussian model. Plotted are observed values as a function of predicted values for the 10th, 50th, and 90th percentiles for each participant-by-angle combination. Overall, the model fits well, certainly as well as other gradual growth models (cf. Ratcliff & Smith, 2004). We note, however, that there is a slight underestimation of inordinately long RTs.

Figure 6B shows averaged estimates of log shape as a function of log scale for the six tilt-angle conditions. The points order by tilt-angle condition with decreasing scales for increasing tilt angles. Log shape not only decreases with log scale, it does so in a manner highly consistent with bound invariance. The dashed line shows the relationship in which the bound is invariant at $\log\lambda = -.085$. The statistical significance of these trends was assessed by submitting participant-by-condition parameter estimates to a

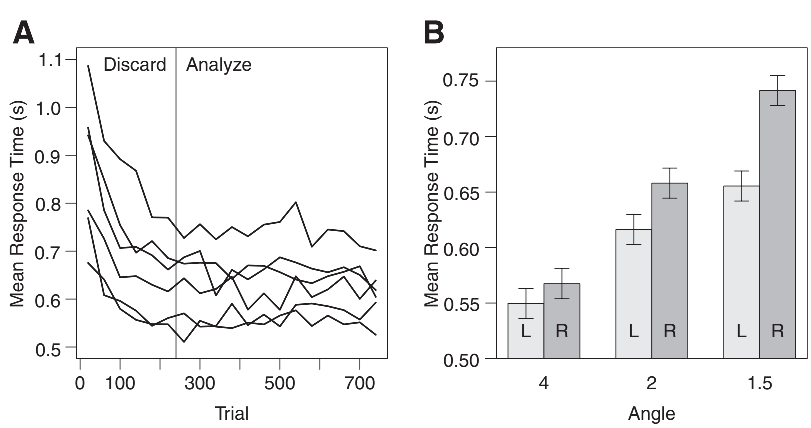

Figure 5. A. Mean response time for the six conditions as a function of practice. Response times decreased within the first 240 trials and remained steady thereafter. B. Mean response time as a function of condition for the analyzed data. Error bars denote 95% within-subject confidence intervals (Masson & Loftus, 2003). L = left; R = right.

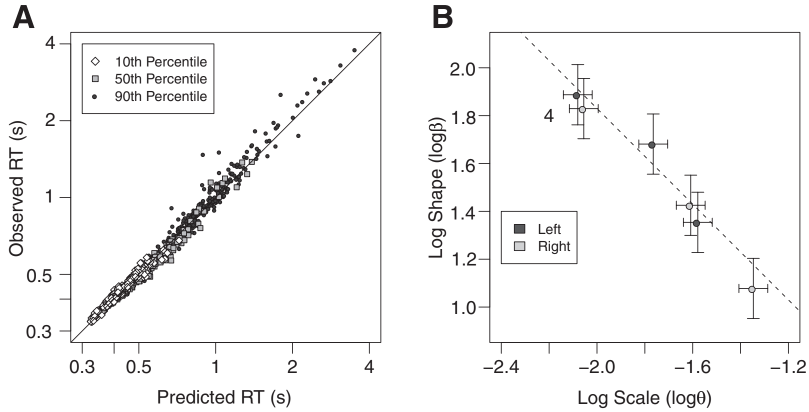

Figure 6. A. The inverse Gaussian model is well specified. Shown are predicted and observed select percentiles for each participant by condition. B. Mean log shape (logβ) as a function of mean log scale (logθ). The dashed line has a slope of −1, the value predicted by bound invariance. Error bars denote 95% within-subject confidence intervals (Masson & Loftus, 2003). RT = response time.

repeated-measures ANOVA. Shape invariance does not hold across the six conditions, $F(5, 285) = 19.8$, $p < .05$. In contrast to shape invariance, bound invariance may not be rejected, $F(5, 285) = 0.60$, $p \approx .7$. Figure 6B also provides some evidence that the slightly elevated error rate for the 1.5° condition is inconsequential. Even if this condition is ignored, the same decrease of log shape is observed.

Figure 6B reveals an unforeseen result about the nature of bias. Participants exhibit an overall bias in that they responded more quickly and more accurately to leftward than rightward tilt angles. This bias is manifest in the drift rates rather than in bounds. It is better characterized as an encoding bias rather than as a response bias (Link, 1992). Gradients were seemingly perceived as slightly more counterclockwise in orientation than as they were displayed.

Conclusions

The observed bound invariance and the observed failure of shape invariance provide clear conclusions. First, the data are highly concordant with the simple one-bound gradual growth model of Figure 1. Second, they are discordant with shape invariance. This last point about the lack of shape invariance is conditional on the inverse Gaussian model, although the inverse-Gaussian model seems reasonable for these data (see Figure 6A). This support for the gradual growth model complements previous research that shows the applicability of the diffusion model to a variety of tasks and further shows that diffusion model parameters may be selectively influenced. In summary, the gradual growth model is preferred even when compared with a flexible alternative that makes highly similar RT predictions.

One limitation of the results is that the analyzed experiment taps fairly low-level processes. Participants decided if the tilt of a grating was leftward or rightward. Such a decision is mostly perceptual and might be made without recourse to substantial semantic or mnemonic processing. Given that diffusion models have accounted for data in tasks with substantial mnemonic and semantic demands such as recognition memory (Ratcliff, 1978; Spaniol et al., 2008) and lexical decision (Ratcliff et al., 2004), it seems plausible that our shape-dependency results may extend to these domains as well. Likewise, it seems unlikely that shape invariance may hold in more complex domains given that it does not hold in simple perceptual ones.

Although shape invariance may not be an exact description of underlying processing, it nonetheless may be useful in certain contexts. Shape invariance may serve as an appropriate statistical model for assessing the effects of covariates such as experimental manipulations and group membership (Rouder et al., 2005; Rouder, Tuerlinckx, Speckman, Lu, & Gomez, 2008; Van Breukelen, 2005). In such models, shift parameters correspond to residual processes such as the execution of responses, and scale parameters describe central decision-making processes. These models are statistically tractable and far more realistic than linear (ANOVA) models of RT. Because of their tractability, they may be more useful than gradual growth models for analyses where there are few observations, many conditions, or few error responses. Researchers using shape invariance as a statistical tool should be mindful that shape invariance holds only approximately, although to a far greater degree than the equal-variance assumption in conventional linear models.

References

Brown, S., & Heathcote, A. (2005). A ballistic model of choice response time. *Psychological Review, 112,* 117–128.

Chhikara, R. S., & Folks, J. L. (1989). *The inverse Gaussian distribution: Theory, methodology, and applications.* New York, NY: Marcel Dekker.

Dolan, C., van der Maas, H., & Molenaar, C. M. (2002). A framework for ML estimation of parameters of (mixtures of) common reaction time distributions given optional truncation or censoring. *Behavioral Research Methods, Instruments, and Computers, 34,* 304–323.

Gomez, P., Ratcliff, R., & Perea, M. (2007). Diffusion model of the go/no-go task. *Journal of Experimental Psychology: General, 136,* 389–413.

Hanes, D. P., & Schall, J. D. (1996, October 18). Neural control of voluntary movement initiation. *Science, 274,* 427–430.

Huk, A., & Shadlen, M. N. (2005). Neural activity in macaque parietal cortex reflects temporal integration of visual motion signals during perceptual decision making. *Journal of Neuroscience, 25,* 10420–10436.

Jiang, Y., Rouder, J. N., & Speckman, P. L. (2004). A note on the sampling properties of the Vincentizing (quantile averaging) procedure. *Journal of Mathematical Psychology, 48,* 186–195.

Laming, D. R. J. (1968). *Information theory of choice-reaction times.* London, United Kingdom: Academic Press.

Link, S. W. (1992). *Wave theory of difference and similarity.* Hillsdale, NJ: Erlbaum.

Logan, G. D. (1992). Shapes of reaction time distributions and shapes of learning curves: A test of the instance theory of automaticity. *Journal of Experimental Psychology: Learning, Memory, and Cognition, 18,* 883–914.

Luce, R. D. (1986). *Response times.* New York, NY: Oxford University Press.

Masson, M. E. J., & Loftus, G. R. (2003). Using confidence intervals for graphically based data interpretation. *Canadian Journal of Experimental Psychology, 57,* 203–220.

Matzke, D., & Wagenmakers, E.-J. (2009). Psychological interpretation of ex-Gaussian and shifted Wald parameters: A diffusion model analysis. *Psychonomic Bulletin and Review, 16,* 798–817.

Morton, J. (1969). The interaction of information in word recognition. *Psychological Review, 76,* 165–178.

Myerson, J., Hale, S., Wagstaff, D., Poon, L. W., & Smith, G. A. (1990). The information-loss model: A mathematical theory of age-related cognitive slowing. *Psychological Review, 97,* 475–487.

Myerson, J., Hale, S., Zheng, Y., Jenkins, L., & Widaman, K. W. (2003). The difference engine: A model of diversity in speeded cognition. *Psychonomic Bulletin and Review, 10,* 262–288.

Rabbitt, P. M. (1966). Errors and error correction in choice-response tasks. *Journal of Experimental Psychology, 71,* 264–272.

Ratcliff, R. (1978). A theory of memory retrieval. *Psychological Review, 85,* 59–108.

Ratcliff, R. (1979). Group reaction time distributions and an analysis of distribution statistics. *Psychological Bulletin, 86,* 446–461.

Ratcliff, R., Gomez, P., & McKoon, G. M. (2004). A diffusion model account of the lexical decision task. *Psychological Review, 111,* 159–182.

Ratcliff, R., & McKoon, G. M. (2008). The diffusion decision model: Theory and data for two-choice decision tasks. *Neural Computation, 20,* 873–922.

Ratcliff, R., & Rouder, J. N. (1998). Modeling response times for decisions between two choices. *Psychological Science, 9,* 347–356.

Ratcliff, R., & Rouder, J. N. (2000). A diffusion model analysis of letter masking. *Journal of Experimental Psychology: Human Perception and Performance, 26,* 127–140.

Ratcliff, R., & Smith, P. L. (2004). A comparison of sequential sampling models for two-choice reaction time. *Psychological Review, 111,* 333–367.

Ratcliff, R., Spieler, D., & McKoon, G. (2000). Explicitly modeling the effects of aging on response time. *Psychonomic Bulletin & Review, 7,* 1–25.

Ratcliff, R., Van Zandt, T., & McKoon, G. (1999). Comparing connectionist and diffusion models of reaction time. *Psychological Review, 106,* 261–300.

Reddi, B., & Carpenter, R. (2003). Accuracy, information and response time in a saccadic decision task. *Journal of Neurophysiology, 90,* 3538–3546.

Rouder, J. N., Lu, J., Speckman, P. L., Sun, D., & Jiang, Y. (2005). A hierarchical model for estimating response time distributions. *Psychonomic Bulletin and Review, 12,* 195–223.

Rouder, J. N., Speckman, P. L., Steinley, D., Pratte, M. S., & Morey, R. D. (2010). A bootstrap test of shape invariance across distributions. In S. Kolenikov, D. Steinley, & L. Thombs (Eds.), *Statistics in the social sciences: Current methodological developments* (pp. 159–174). New York, NY: Wiley.

Rouder, J. N., Tuerlinckx, F., Speckman, P. L., Lu, J., & Gomez, P. (2008). A hierarchical approach for fitting curves to response time measurements. *Psychonomic Bulletin & Review, 15,* 1201–1208.

Smith, G. A., & Brewer, N. (1995). Slowness and age: Speed–accuracy mechanisms. *Psychology and Aging, 10,* 238—247.

Spaniol, J., Voss, A., & Grady, C. L. (2008). Aging and emotional memory: Cognitive mechanisms underlying the positivity effect. *Psychology and Aging, 23,* 859–872.

Thapar, A., Ratcliff, R., & McKoon, G. M. (2003). A diffusion model analysis of the effects of aging on letter discrimination. *Psychology and Aging, 18,* 415–429.

Ulrich, R., & Miller, J. O. (1993). Information processing models generating lognormally distributed reaction times. *Journal of Mathematical Psychology, 37,* 513–525.

Usher, M., & McClelland, J. L. (2001). On the time course of perceptual choice: The leaky competing accumulator model. *Psychological Review, 108,* 550–592.

Van Breukelen, G. J. P. (2005). Psychometric modeling of response time and accuracy with mixed and conditional regression. *Psychometrika, 70,* 359–376.

Voss, A., Rothermund, K., & Voss, J. (2004). Interpreting the parameters of the diffusion model: An empirical validation. *Memory & Cognition, 32,* 1206–1220.

Wagenmakers, E.-J., & Brown, S. (2007). On the linear relation between the mean and the standard deviation of a response time distribution. *Psychological Review, 114,* 830–841.

(*Appendix follows*)

Appendix

Statistical Analysis

A mixture model was used to estimate inverse Gaussian scale and shape parameters. Each observation was assumed to be from one of two sources: (a) the process of interest, which is distributed as an inverse Gaussian, or (b) an outlier distribution, which is distributed as a continuous uniform on the interval 0–5 s (Dolan, van der Maas, & Molenaar, 2002). The uniform allows for outliers that are potentially faster as well as slower than the process of interest. This property seems appropriate as there are observations that are exceedingly slow and exceedingly fast.

Let y_{ijkm} denote the mth replicate for the ith participant observing the jth tilt direction (left or right) and kth magnitude ($i = 1, \ldots, I$, where I denotes the number of participants; $j = 1, 2$; $k = 1, 2, 3$; and $m = 1, \ldots, M_{ijk}$, where M_{ijk} denotes the number of replicates). Let z_{ijkm} be a latent indicator that takes a value 1 when y_{ijkm} is from the process of interest and value 0 otherwise. Then,

$$y_{ijkm} | z_{ijkm}, \psi_{ij}, \theta_{ijk}, \beta_{ijk} \overset{ind}{\sim} \begin{cases} \text{Inverse Gaussian}(\psi_{ij}, \theta_{ijk}, \beta_{ijk}), & z_{ijkm} = 1, \\ \text{Uniform}(0, 5), & z_{ijkm} = 0, \end{cases}$$

where

$$z_{ijkm} \overset{iid}{\sim} \text{Bernoulli}(\pi).$$

The inverse Gaussian distribution has a shift–scale–shape parameterization. Note that scale (θ_{ijk}) and shape (β_{ijk}) are free to vary across participants, tilt direction, and tilt magnitude without constraint. Shift (ψ_{ij}) varies across participants and tilt direction but not across magnitude. Typically, shifts are not considered a function of stimulus condition as they represent nondecision latencies (see Ratcliff & Rouder, 1998). There is the concern, however, that differences in dexterity across response hands could affect the assessment of distributional shape. This difference may be modeled by allowing for unique shift parameters for each hand-by-participant combination. In the current analysis, which includes only correct responses, left-hand responses arise only from left tilt angles, and right-hand responses arise only from right tilt angles. Therefore, differences in dexterity across response hands may be accounted for by including a unique ψ_{ij} for each participant-by-angle-direction combination.

Analysis was performed with Bayesian Markov chain Monte Carlo methods, and posterior means served as point estimates. With such methods, priors are needed on all parameters. Priors were chosen to be vague and convey only a minimal degree of information. Priors on all ψ_{ij} were flat (noninformative); priors on all θ_{ijk} were lognormal with mean and variance on $\log(\theta_{ijk})$ of –1.2 and 1.0, respectively. This prior distribution is broad with substantial mass from a few milliseconds to several seconds. Priors on all β_{ijk} were gamma with a shape of 2 and a rate of 0.3, and these have substantial mass on reasonable shape values from 0.5 to 20. The prior on π, the mixing probability, was flat on [0,1]. To test whether the reported results are robust to different choices, we reanalyzed the model with several different priors. Additionally, we reanalyzed the model with priors placed on drift rate and bound rather than on scale and shape. There is only a marginal effect of prior specification on parameter estimates, indicating that priors do not have undue influence on estimates.

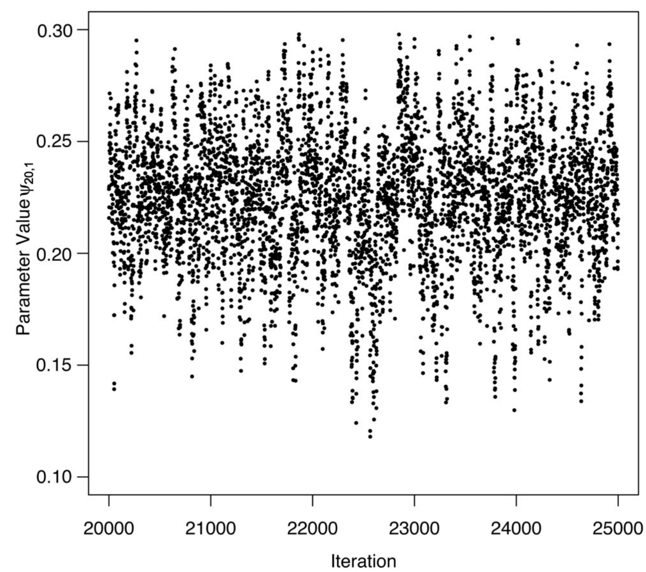

Figure A1. Markov chain Monte Carlo outputs after thinning for parameter $\psi_{20,1}$, one of the more slowly converging parameters. There are 50,000 values in the thinned chains, and the figure shows the values from 20,000 to 25,000.

One issue in analysis is convergence of samples of posterior distributions. The Markov chains display a substantial degree of autocorrelation. To ensure convergence, we ran chains for 500,000 iterations and thinned them by a multiple of 10. Figure A1 shows a small part of a sample chain after thinning; autocorrelation is still present, but its effects on posterior mean estimates are mitigated by the large number of iterations.

Figure 6A shows the adequacy of the model. Although the model fits very well for the vast majority of observations, there is a small underestimation of very long responses. Given the coarse nature of the mixture model, in which there is a single outlier distribution across all individuals and angles, this small degree of misspecification is not surprising. We have analyzed several other mixture models with alternative specifications of outliers, including a model with no outlier distribution. Although the choice of outlier distribution affects the quality of the fits, it does not affect much the assessment of shape versus bound invariance. In all cases, bound invariance held and shape invariance was violated. Hence, bound invariance appears to be a robust property of these data.

Received December 31, 2009
Revision received May 27, 2010
Accepted May 28, 2010 ■